2004

Noble Metal Nanostructures Synthesized inside Mesoporous Nanotemplate Pores

J. Arbiol

E. Rossinyol

A. Cabot

F. Peiró

A. Cornet

See next page for additional authors

Publication Info

Published in *Electrochemical and Solid-State Letters*, Volume 7, Issue 7, 2004, pages J17-J19.

Publisher's Version: http://dx.doi.org/10.1149/1.1724827
Arbiol, J., Rossinyol, E., Cabot, A., Peiro, F., Cornet, A., Morante, J. R., Chen, F., & Liu, M. (2004). Nobel Metal Nanostructures Synthesized inside Mesoporous Nanotemplate Pores. Electrochemical and Solid-State Letters, 7 (7), J17 – J19. http://dx.doi.org/10.1149/1.1724827

Electrochemical and Solid-State Letters, **7** (7) J17-J19 (2004)
0013-4651/2004/7(7)/J17/3/$7.00 © The Electrochemical Society, Inc.

Noble Metal Nanostructures Synthesized inside Mesoporous Nanotemplate Pores

J. Arbiol,[a,z] E. Rossinyol,[a] A. Cabot,[a] F. Peiró,[a] A. Cornet,[a] J. R. Morante,[a,*] Fanglin Chen,[b,*] and Meilin Liu[b,*]

[a]*EME Enginyeria i Materials Electrònics, Departament d'Electrònica, Universitat de Barcelona, E-08028 Barcelona, Spain*
[b]*School of Materials Science and Engineering, Georgia Institute of Technology, Atlanta, Georgia 30332-0245, USA*

Noble metal impregnation has resulted in the inclusion of metal nanostructures within the SBA-15 mesoporous silica hexagonal pores (from nanoclusters to nanowires). A bright-field transmission electron microscopy three-dimensional reconstruction is proposed to analyze the localization of nanostructures within the pores of mesoporous nanotemplates. The method allows corroboration whether the nanostructures are synthesized inside the pores or they are synthesized alternatively on the nanotemplate aggregates exterior surface.
 [DOI: 10.1149/1.1724827]

Manuscript submitted October 31, 2003; revised manuscript received November 21, 2003. Available electronically April 26, 2004.

In recent years, mesoporous materials have attracted much attention for the development of catalytic applications because of their extremely high surface areas. [1,2] The physical and chemical properties of these mesoporous materials can be modified dramatically by incorporation of noble metals or metal oxides to decorate the surfaces.[3-6] In previous works, we reported our initial results using SBA-15 mesoporous silica as a novel selective filter for gas sensors.[7-9] We showed how a SnO_2-based, thick-film gas sensor showed greatly improved selectivity to CH_4 in CH_4-CO gas mixtures when the sensor was covered with a layer of Pt/Pd loaded mesoporous silica.[8] Moreover, mesoporous materials have recently been used as nanotemplates controlling the morphology of the nanostructures synthesized inside their pores.[10,11] In this way, the distributions of Pt and Pd nanostructures (from nanoclusters to nanowires) in SBA-15 mesoporous SiO_2 nanotemplates have been reported elsewhere.[7] In previous works, however, it was assumed, not yet confirmed, that Pt and Pd were within the silica hexagonal pores. Previous structural studies were based on conventional transmission electron microscopy (TEM) techniques, which give a two-dimensional (2-D) projection image of an object under study. In this communication, we report our findings in further structural characterization of noble metal-loaded mesoporous structures. Bright-field 3-D TEM reconstruction has been proposed to analyze the localization of nanostructures within the pores of mesoporous nanotemplates. The method allows one to corroborate whether the nanostructures are synthesized inside the pores or they are synthesized alternatively on the nanotemplate aggregates exterior surface. As an example we show how noble metal impregnation has resulted in the inclusion of metal nanostructures within the SBA-15 mesoporous silica hexagonal pores (from nanoclusters to nanowires).

SBA-15 mesoporous silica was synthesized following the procedure reported by Zhao *et al.*[12,13] using pluronic P123 triblock copolymer ($EO_{20}PO_{70}EO_{20}$) as the structure-directing agent. Noble metal additives were introduced into mesoporous silica by impregnation of the SBA-15 silica with 0.01 M aqueous solution of palladium chloride and ammonium tetrachloroplatinate, followed by slow evaporation of water. For TEM observations, mesoporous silica powders were dispersed ultrasonically in *n*-hexane and deposited on amorphous holey carbon membranes. Conventional TEM was performed using a Philips CM30 SuperTwin electron microscope operated at 300 keV. A series of images with different degrees of tilt for 3-D reconstruction were obtained in a JEOL 1010 electron microscope operated at 100 keV, with a high angle tilt holder $\pm$ 60°.

Among the three main classes of mesoporous molecular sieves (MMS),[2] SBA-15 mesoporous silica is thermally the most stable one because it has long-range order, large pores of uniform pore size, and thick walls. The obtained material has a hexagonal array of mesopores with a controlled variable lattice constant from 8 to 12 nm. The mesopores are arranged in structures groupings few hundred pores with lengths up to 2 μm (Fig. 1 and 2).

The obtained mesoporous templates were loaded with noble metal compounds, such as Pd and Pt. Extensive TEM studies of the noble metal impregnated mesoporous silica indicated that Pd and Pt could be deposited at two different locations. Noble metal was found forming metal nanoclusters on the surface of the mesoporous silica. Noble metal seemed to be placed along the silica mesopores as small nanoclusters for low metal loadings (Fig. 1) or as noble metal hexagonal prisms (nanowire-like structures) occupying the entire pores for high metal loadings (Fig. 2).[7] In this latest case, we could not prove that the nanoclusters and nanowires were placed within the pores, as the TEM images give only a 2-D projection image of the material. At this point, it would be interesting to demonstrate the inclusion of the noble metal inside the pores for two main reasons: (*i*) to show the availability of mesoporous silica as a novel promising nanotemplate and (*ii*) to indicate that the whole surface area of the mesoporous aggregates is available for catalytic purposes, reaching large active surface areas, up to 800 m^2/g. To confirm the location of the noble metal clusters introduced by solution impregnation, we applied the 3-D TEM reconstruction technique. This methodology has been used largely as a powerful analysis of biological molecules since the late 1960s,[14] and is now being used as a standard tool for analysis of macromolecules with nanometric resolution.[15] However, the TEM 3-D characterization has only recently been used in materials science, and especially on catalysts.[16] The main reason why this technique has not been used extensively in physical sciences is because bright-field (BF) TEM 3-D reconstruction is generally unsuitable for crystalline specimens.[17] In this way, Weyland *et al.* seemed to have solved this problem using high-angle annular dark-field (HAADF) tomography in a scanning transmission electron microscope (STEM).[17,18] However, in our case, we can use BF TEM, as our silica mesoporous nanotemplates are not crystalline.

Attending to this methodology, we can obtain a 3-D reconstruction of a noncrystalline object by acquiring TEM BF micrographs at a large tilt angle range, from 60 to −60° (Fig. 3). Each 2-D TEM micrograph acts as a projection slice of the final 3-D reconstruction. In Fig. 3, one of the selected mesoporous silica aggregates is shown. In this case, the aggregate was loaded with Pt. In the main picture the noble metal nanostructures have been marked with black arrows that are followed during 3-D reconstruction to confirm that the inclusion of the noble metals are within the pores. The first nanostructure marked was defined in a previous work,[7] as a metal nanowire synthesized inside the silica pores (NW). The second nanostructure

* Electrochemical Society Active Member.
z E-mail: arbiol@el.ub.es

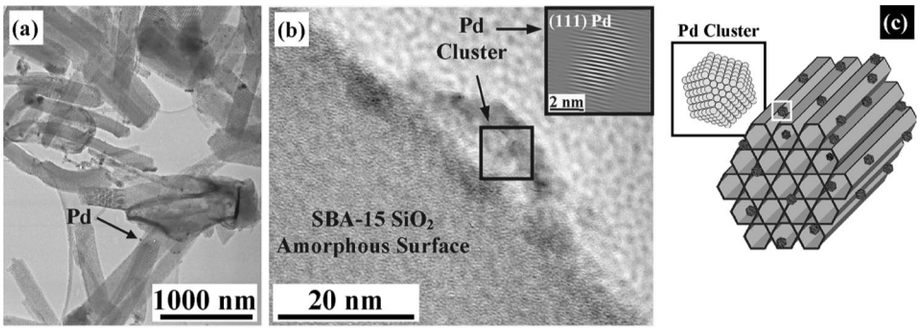

Figure 1. (a) General TEM view of the Pd-modified silica mesoporous material. (b) HRTEM micrograph of a Pd nanocluster placed on the mesoporous surface. The inset shows the filtered Pd (111) planes of the selected nanocluster. (c) Model proposed for the nanocluster dispersion in the Pd-modified mesoporous silica. Nanoclusters used in the model are the 561 atom Pd cuboctahedrons (with ~ 3 nm lateral size).

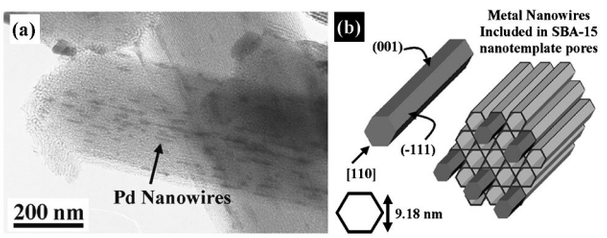

Figure 2. (a) 2-D bright-field TEM view of a Pd-modified SBA-15 silica mesoporous aggregate. (b) Pd-modified SBA-15 mesoporous silica model with platinum adopting nonregular hexagonal prism morphology.

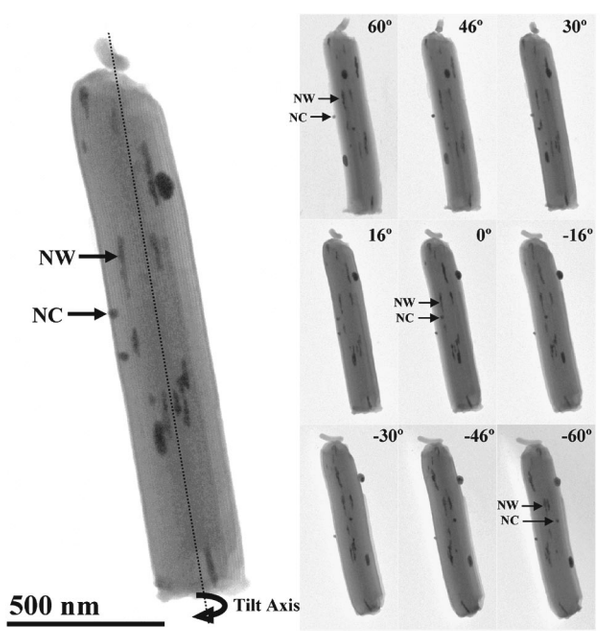

Figure 3. The main image shows a Pt-modified SBA-15 silica mesoporous aggregate. Marked with the black arrows are two of the characteristic noble metal nanostructures found in these materials. NW represents a noble metal nanowire and NC corresponds to a surface nanocluster. On the right side we show some of the 2-D TEM micrographs used as 2-D slices to compose the 3-D TEM reconstruction. On those 2-D slices from 60 to −60° we can follow the rotation of the noble metal nanostructures selected, NC and NW.

marked was defined as a surface nanocluster (NC). On the right, are presented some TEM tilt slices. Looking at the first tilted micrograph (60° tilt), note the selected nanocluster, marked as NC, is placed on the left side border of the mesoporous aggregate, which clearly indicates that this cluster is definitely placed on the outside surface of the silica aggregate. The Pt nanowire, marked as NW, is placed in the middle of the mesoporous aggregate. Using this 2-D tilted slice, one cannot differentiate whether the noble metal NW is placed on the surface, or inside the pores. If one follows both nanostructures along the different tilted 2-D slices, one finds that the NC shows a large radius rotation along the silica aggregate surface perimeter while the NW shows a low radius rotation. On the last TEM tilt slice, obtained at − 60°, one finds that the NC is almost placed at the right side border of the mesoporous aggregate. This movement is in good agreement with a 120° rotation along the aggregate surface perimeter. At the −60° tilt slice, the NW remains almost in the center of the aggregate. The low radius rotation of the Pt NW demonstrates that it must be placed within the central pores of the silica aggregate, which confirms the assumptions made in our previous work.[7] A complete animated 3-D TEM reconstruction of the mesoporous aggregate loaded with Pt is available at

http://nun97.el.ub.es/~arbiol/discdos/nanopart/web/Tomo/Model_1.html

At this address one can observe the rotation of both NW and NC nanostructures in 3-D live motion.

Concerning the technological applications of these materials, we showed that inserting noble metal nanoclusters of 1-3 nm in the pores, improved the catalytically active surface area, taking advantage of the pore internal surfaces.[7] However, if a high amount of noble metal is loaded inside the pores, the formation of hexagonal prisms that could block the gas paths through the mesoporous structures were obtained. Although this latest option is undesirable for gas filters, we can take advantage of this phenomenon and use the mesoporous silica as an excellent novel nanotemplate for metal nanowire production.[10] At this point, it should be assured that the noble metal loading occurs effectively inside the pores. In this work we have accounted for this by BF 3-D TEM reconstruction. Once the nanowires are formed inside the pores, the porous SiO_2 network can be chemically removed, yielding metal nanowires.

Acknowledgments

This work has been done in the facilities of the Serveis Científicotecnics of Universitat de Barcelona, in the frame of the activities of the Reference Center on Advanced Materials for Energy (CERMAE) of Generalitat de Catalunya. The authors also gratefully acknowledge partial support of this project by the Georgia Institute of Technology Molecular Design Institute, under prime contract N00014-95-1-1116 from the U.S. Office of Naval Research.

The University of Barcelona assisted in meeting the publication costs of this article.

References

1. S. H. Joo, S. J. Choi, I. Oh, J. Kwak, Z. Liu, O. Terasaki, and R. Ryoo, *Nature (London)*, **412**, 169 (2001).
2. D. Trong On, D. Desplantier-Giscard, C. Danumah, and S. Kaliaguine, *Appl. Catal., A* **222**, 299 (2001).
3. K. Kageyama, J. Tamazawa, and T. Aida, *Science*, **285**, 2113 (1999).
4. W. Zhou, J. M. Thomas, D. S. Shephard, B. F. G. Johnson, D. Ozkaya, T. Maschmeyer, R. G. Bell, and Q. Ge, *Science*, **280**, 705 (1998).
5. W. Cai, Y. Zhang, J. Jia, and L. Zhang, *Appl. Phys. Lett.*, **73**, 2709 (1998).
6. J. V. Ryan, A. D. Berry, M. L. Anderson, J. W. Long, R. M. Stroud, V. M. Cepak, V. M. Browning, D. R. Rolison, and C. I. Merzbacher, *Nature (London)*, **406**, 169 (2000).
7. J. Arbiol, A. Cabot, J. R. Morante, F. Chen, and M. Liu, *Appl. Phys. Lett.*, **81**, 3449 (2002).
8. A. Cabot, J. Arbiol, A. Cornet, J. R. Morante, F. Chen, and M. Liu, *Thin Solid Films*, **436**, 64 (2003).
9. A. Cabot, J. Arbiol, E. Rossinyol, J. R. Morante, F. Chen, and M. Liu, *Electrochem. Solid-State Lett.*, **7** G93 (2004).
10. Y.-J. Han, J. M. Kim, and G. D. Stucky, *Chem. Mater.*, **12**, 2068 (2000).
11. H. Wenchong, G. Dawei, C. Zhi, Y. Liming, S. Kozo, G. Craig, and K. Padmakar, *Appl. Phys. Lett.*, **79**, 3083 (2001).
12. D. Zhao, Q. Huo, J. Feng, B. F. Chmelka, and G. D. Stucky, *J. Am. Chem. Soc.*, **120**, 6024 (1998).
13. D. Zhao, J. Feng, Q. Huo, N. Melosh, G. H. Fredrickson, B. F. Chmelka, and G. D. Stucky, *Science*, **279**, 548 (1998).
14. D. J. De Rosier, and A. Klug, *Nature (London)*, **217**, 130 (1968).
15. A. J. Koster, R. Grimm, D. Typke, R. Hegrel, A. Stoschek, J. Walz, and W. Baumeister, *J. Struct. Biol.*, **120**, 276 (1997).
16. A. J. Koster, U. Ziese, A. J. Verkleij, A. H. Janssen, and K. P. de Jong, *J. Phys. Chem. B*, **104**, 9368 (2000).
17. M. Weyland, *Top. Catal.*, **21**, 175 (2002).
18. P. A. Midgley, M. Weyland, J. M. Thomas, and B. F. G. Johnson, *Chem. Commun. (Cambridge)*, **2001**, 907.